

Article

Geochemical Modeling of Changes in Storage Rock Environments at CO₂ Injection Sites

Monika Licbinska ¹, Lenka Mertova ¹, Nada Rapantova ² and Katerina Stejskalova ^{2,*}

¹ Faculty of Mining and Geology, VSB-Technical University of Ostrava, 17. Listopadu 15, 70800 Ostrava-Poruba, Czech Republic

² Faculty of Civil Engineering, VSB-Technical University of Ostrava, 17. Listopadu 15, 70800 Ostrava-Poruba, Czech Republic

* Correspondence: katerina.stejskalova@vsb.cz; Tel.: +420-596-991-360

Abstract: Geochemical modeling in TOUGHREACT code was used to simulate chemical processes in CO₂–rock–brackish water systems in a pilot research environment of CO₂ storage in the Brodské area (Czech Republic). Models studied mineralogical changes in rock samples resulting from acidification of the aqueous phase caused by the dissolution of pressurized supercritical CO₂. Rock samples of the reservoir horizon and cement from the grouting of an injection borehole were considered, and the water phase represented the mineralized groundwater. The aim of the study was to characterize the influence of CO₂ in the geological structure on mineralogical rock changes and to predict gas distribution through the rocks bearing brackish water. The most important chemical processes are dissolution of carbonates and clay minerals during the injection of CO₂ into the structure, as the increase in porosity in the structure affects the sequestration capacity of the reservoir rock. In the CO₂–cement–brackish water system, the models confirm the rapid dissolution of portlandite and its replacement with calcite. The CSH gel is also dissolved, and silica gel appears. The porosity of the cement decreases. Further studies on such a cement slurry are needed to prevent the possibility of mechanical damage to the integrity of the borehole.

Keywords: CO₂ injection; geochemical modeling; TOUGHREACT; Labský horizon; Portland cement; brackish water



Citation: Licbinska, M.; Mertova, L.; Rapantova, N.; Stejskalova, K. Geochemical Modeling of Changes in Storage Rock Environments at CO₂ Injection Sites. *Minerals* **2023**, *13*, 298. <https://doi.org/10.3390/min13020298>

Academic Editor: Rafael Santos

Received: 12 December 2022

Revised: 14 February 2023

Accepted: 15 February 2023

Published: 20 February 2023



Copyright: © 2023 by the authors. Licensee MDPI, Basel, Switzerland. This article is an open access article distributed under the terms and conditions of the Creative Commons Attribution (CC BY) license (<https://creativecommons.org/licenses/by/4.0/>).

1. Introduction

Several publications on carbon capture and storage (CCS) mention and detail specific experiments that precede the implementation of CCS in various geological structures [1–6]. Experiments with mixed fluids between supercritical CO₂ and saline NaCl have been described [7–9]. Experiments have shown that the injection of CO₂ into the rock system leads to complex and significant changes in the nature of such a system. One of many accompanying phenomena is, for example, the nucleation and growth of new carbonate and silicate minerals [9–11]. The accompanying phenomenon is a change in the permeability of the storage reservoir structure, which may have a negative impact on the entire storage system.

The same has been demonstrated in experiments simulating P-T conditions of real potential storage. It turns out that the interaction between the CO₂–H₂O system of sedimentary rock with carbonate cement leads to the dissolution and re-formation of carbonate minerals [12,13]. The study of Brandl et al. [14] also mentions the reduction of porosity near injection boreholes. Clogging involves reactions between carbonates, clay and related minerals, oxides, hydroxides, and iron sulfides. A significant, and in some cases essential, source component for the formation of clogging minerals is the borehole’s own material, the grouting [15,16]. Crystallization processes are controlled mainly by the partial pressure of CO₂, pH, and groundwater flow [17,18]. Oxidation–reduction reactions of iron are also of major importance.

Processes occurring in the environment of the reservoir after CO₂ injections have been clearly and conclusively described in many articles [3–6], particularly those relating to geochemical changes in both the reservoir and the overlying confining layer [1,2,4]. Changes in minerals and pore space can affect storage capacity and injectivity in the short term; in the long run, they affect the distribution of individual phases (fluids, rocks) [3,13]. Therefore, it is necessary to model the various aspects of these processes, both at the microscale (e.g., changes in minerals and pore space) and at the macroscale (e.g., the development of new preferential migration pathways due to the dissolution of minerals, fluid quality changes, etc.). Geochemical modeling of rock alterations is therefore a key supportive method for assessing the safe operation of future storage [6]. This study is focused on simulating chemical processes in CO₂–rock–brackish water systems in a pilot research environment of CO₂ storage in the Brodske area (South Moravia, Czech Republic). This location is an extracted oil deposit and is potentially suitable for CO₂ injection.

2. Materials and Methods

Models involving kinetic transport through porous media and thermodynamic issues of multiphase systems are very useful in forecasting the impact of CO₂ injections on the changes to the rock environment at the site. These models are based on information regarding petrophysical, mineralogical, and hydrogeological characteristics of porous media, hydrochemical analysis of fluid composition, pressure and temperature values of the deposit, and kinetic parameters.

2.1. Input Parameters for the Model

A model of reservoir rocks of the Labsky horizon (labeled Br-52) from the locality of Brodske was considered. A description of the rock is given in Table 1. The Labsky horizon lies at a depth of about 1000 m and is formed by a Miocene sandstone about 15.5 million years old (stratigraphically belonging to the Middle Badenian). A Br-52 sample is considered a representative sample of the rock of the storage reservoir. It is a mid-Badenian medium-grained sandstone located at a depth of 1150 m, from what is called the Labsky horizon.

Table 1. The samples of reservoir rocks.

Borehole	True Vertical Depth (m)	Stratigraphy	Lithology
Br-52	1150–1155	STBA* Reservoir	Medium-grained calcareous sandstone

*STBA—Middle Badenian.

As a sample of the water phase, which forms the filling of the pore space of the reservoir formation in the so-called Labsky horizon, the water solution from the Br-45 borehole was used. The water sample from the aquifer was taken by the project partner (MND Energie a.s.) from a depth of 1105 m and the chemical analysis of the water was carried out in the laboratories of the ÚJV Řež, a.s. near Prague. Thereafter, synthetic water was produced in the same laboratory, and its chemistry corresponded to the water composition in the aquifer. The chemical composition of this solution is shown in Table 2.

For modeling changes in the rock environment, it was also necessary to consider the entry of a gaseous CO₂ phase which, under the bearing horizon conditions (temperature: 43 °C, pressure: 116 bar), achieves a supercritical state with a resulting equilibrium partial pressure (P_{CO₂}) of approximately 115.5 bar. These values were determined by the project partner (MND Energie a.s., Hodonin, Czech Republic) and were based on values monitored directly on site.

Table 2. Physico-chemical parameters of synthetic brackish water Br-45.

Synthetic Water Br-45		
Ca ²⁺	(mg/L)	142.9
Mg ²⁺	(mg/L)	55.2
Na ⁺	(mg/L)	3777.0
K ⁺	(mg/L)	84.6
Cl ⁻	(mg/L)	4826.2
HCO ₃ ⁻	(mg/L)	1410.9
SO ₄ ²⁻	(mg/L)	785.9
TDS *	(mg/L)	10,998.1
Other parameters		
T *	(°C)	43
pH	-	8.1
I *	mol/L	0.21
depth	meter	1105

* TDS—total dissolved substances; T—temperature; I—ionic strength.

The mineralogical and petrophysical properties of the studied rock sample, the characteristics of the cement in the boreholes, and the hydrogeological parameters of the reservoir at the location in question are described in Tables 3–5, respectively.

Table 3. Mineralogical composition of the studied rock sample (wt%) and conversion to percentages by volume (vol.%).

Borehole	Q	Mu	Mic	Chl	Calc	Dol	Alb	Gyp	Porosity	Specific Surface
	(wt%)	(%)	(m ² /g)							
Br-52	60.22	9.83	3.85	6.42	6.97	3.12	7.66	1.92	24.51	0.88
	(vol.%)	(%)								
	46.52	7.10	3.08	3.97	5.26	2.23	6.00	1.33	24.51	

Q—quartz, Mu—muscovite, Mi—microcline, Ka—kaolinite, Chl—chlorite, Calc—calcite, Sid—siderite, Dol—dolomite, Alb—albite, Gyp—gypsum.

Table 4. Mineralogical composition of the cement sample (wt%) and conversion to percentages by volume (vol.%).

Mineral	Formula	wt%	vol.%
CSH1.6	Ca _{1.6} SiO _{3.6} :2.58H ₂ O	42.3	27.43
Portlandite	Ca(OH) ₂	25.2	18.79
Ettringite	Ca ₆ Al ₂ (SO ₄) ₃ (OH) ₁₂ :26H ₂ O	18.2	9.94
Hydrotalcite	Mg ₄ Al ₂ O ₇ :10H ₂ O	5.9	3.89
Katoite-Si	Ca ₃ Al ₂ SiO ₄ (OH) ₈	5.7	7.56
C3FH6	Ca ₃ Fe ₂ (OH) ₁₂	1.9	3.96
Calcite	CaCO ₃	0.8	0.43

The mineralogical composition of Br-52 samples was determined by XRD analysis. XRD powder data were measured at room temperature on a Bruker AXS D8 θ - θ powder diffractometer (Karlsruhe, Germany) in Bragg–Brentano parafocusing geometry using CoK α wavelength ($\lambda = 1.7903 \text{ \AA}$, U = 34 kV, I = 30 mA). Porosity was determined using Hg-porosimetry, and the specific surface area was found by the N₂-BET method by adsorption–desorption isotherms. The samples from borehole Br-52 were part of the drill core and came from depths corresponding to the reservoir rock.

Table 5. Hydrogeological parameters of reservoir rock with medium-grained calcareous sandstone.

Parameters	Value	Unit
thickness	20	m
porosity	24.5	%
horizontal permeability k_R	450	mD
vertical permeability k_z	4.5	mD
pressure P	116	bar
temperature T	43	°C
max. salinity S	72	g/L
CO ₂ density	195	kg/m ³
CO ₂ viscosity	1.5×10^{-4}	Pa·s

The use of classic Portland cement CEM II/B-M (S-V) 32.5R is assumed for the equipped of boreholes through which CO₂ will be injected into the structure. The main component of the cement is Ca–Si hydrate (CSH1.6) [11,19]. The composition of the cement, reported in the literature [11,19,20], corresponds to the analysis of the real sample (sample of Portland cement from borehole Br-52 equipment) used in the model. The mineralogical composition of the cement sample in wt% and vol.% is shown in Table 4.

The hydrogeological parameters of the Labsky horizon are important for understanding and predicting changes in the storage area. These parameters are summarized in Table 5. It is assumed that there is higher horizontal permeability k_R than vertical permeability k_z due to the geological processes undergone during sedimentation. These data were taken from the project partners, and they published their results in a scientific journal [13]. In agreement with Wertz et al. [13], we assumed that due to geological processes undergone during sedimentation, the horizontal perm is 100 higher than the vertical perm. The density and viscosity of CO₂ are dynamically determined in the TOUGHREACT program by the ECO2N module as a function of pressure P, temperature T, and salinity S [21,22].

During the modeling of the spread of injected CO₂ using hydrogeological parameters, an z - x coordinate cylinder was considered, where the x -axis is the distance from the borehole in kilometers, and the z -axis is the thickness of the reservoir. The x -axis is 6 km long and the z -axis is 20 m thick. The network is made up of 193 cells with an exponentially increasing radius. Models were developed in TOUGHREACT (with ECO2N) [22]. The porosity was assumed to be homogeneous throughout the reservoir. The calculations were performed based on the Darcian flow in a porous environment. In the calculations, the amount of CO₂ injected into the reservoir was 8750 tCO₂/year. This parameter was determined by the project partner (MND Energie a.s.).

The fluid dynamic model and the geochemical simulations of mineralogical rock changes were implemented separately.

2.2. Geochemical Modeling

The applied models specified below were designed to describe processes with (a) a short injection time (i.e., dynamic 1-year simulations of instantaneous chemical change in the reservoir affected by the start of CO₂ injection), (b) a longer-term reactivity of CO₂ with the rock environment (6 or 8 years of injection of CO₂ into the storage site), and (c) a long-term period of storage relaxation after the injection (500 years).

The results presented in the following chapter are the outputs of equilibrium, kinetic, and multiphase modeling of the geochemical reactivity of the CO₂–water–rock system, determining the influence of CO₂ on the porosity in the near field of the injection borehole.

Equilibrium models were designed to evaluate changes in porous water chemistry after CO₂ injection into the reservoir to express balances in the rock–CO₂–brackish water system, and to express the solubility of CO₂ in brackish water Br-45. Kinetic and multiphase modeling was conducted to evaluate hydrogeochemical changes in the studied formation in relation to the injection and storage of CO₂ in the structure. This allowed for the assessment

of volumes and quantities of precipitated or dissolved mineral phases and of their impact on reservoir rock permeability in relation to the prediction of possible CO₂-related risks.

TOUGHREACT, The Geochemist's Workbench, and PHREEQC modeling programs were used to meet the above objectives. Modeling systems for the TOUGHREACT multi-phase modeling included the ECO2N Thermodynamic Module. Supporting kinetic and thermodynamic models were applied using The Geochemist's Workbench (GWB) Release 6.0 [23] and additional equilibrium calculations were performed in the PHREEQC program (version 3).

The thermodynamic databases "thermo.dat" (built in the GWB package), the PHREEQC database [24], and the THERMODEM database [25,26] were used.

3. Results and Discussion

3.1. Changes in Br-45 Brackish Water Chemistry after CO₂ Injection

The reaction of CO₂ with groundwater and its effects on potential storage are of utmost importance for the process of mineral sequestration because only a dissolved form of CO₂ can react with the rock. CO₂ solubility is a function of the temperature, pressure, and salinity of the solution, with CO₂ solubility decreasing with increases in the temperature and molarity of the solution, while CO₂ solubility increases with increasing pressure. The dissolution was carried out until the thermodynamic equilibrium was reached and the solution was saturated with CO₂. Based on the input parameters used in the PHREEQC model (Br-45 brackish water chemistry, P_{CO₂} = 116 bar, and temperature = 43 °C), we report the theoretical acidification of Br-45 brackish water as a result of CO₂ injection and calculated chemistry changes in Table 6. The HCO₃⁻ ion is the dominant carbonate component in the solution at alkaline pH. When the pH drops to the acidic values, the bicarbonate ions decrease in solution and carbonic acid, respectively, and CO₂ (aq) [18,27] becomes the dominant carbonate component.

Table 6. Original and model-calculated acidification of Br-45 brackish water.

		Original Br-45	Acidified Br-45
Ca ²⁺	(mg/L)	142.9	142.48
Mg ²⁺	(mg/L)	55.2	55.03
Na ⁺	(mg/L)	3777.0	3765.76
K ⁺	(mg/L)	84.6	83.8
Cl ⁻	(mg/L)	4826.2	4867.7
HCO ₃ ⁻ / CO ₂ (aq)	(mg/L)	1410.9	113,021.26
SO ₄ ²⁻	(mg/L)	785.9	783.56
TDS	(g/L)	10,998.1	10,998.1
Other parameters			
T	(°C)	43	43
pH	-	8.1	4.1
I	mol/L	0.21	0.18

log P_{CO₂} = 2.065.

The change in the character of the input water after CO₂ injection calculated in the PHREEQC program corresponds to the chemical changes of the original water as modified by the TOUGHREACT program in its first-time step. The differentiated chemistry of Br-45 brackish water is then used in simulations in this program as its next steps.

The calculations in PHREEQC were carried out to confirm the changes in the chemistry of the input water.

The process of dissolving CO₂ in a brackish water solution results in the dissolution of certain minerals of the geological environment in which the CO₂ is injected and then is followed by the precipitation of new minerals. This can ultimately lead to changes in the permeability of the rock environment and to a reduction in the capacity of the injected CO₂.

3.2. Modelled Spreading of the Injected CO₂ in Potential Storage

The modeled spread of injected CO₂ in the potential storage is presented in this chapter during the ongoing CO₂ injection period (for the first year and 6 years). The saturation of the environment with the injected gas after the end of the injection is shown here after 100 and 500 years.

Figure 1 is a model showing the evolution of CO₂ pressure in the reservoir and the saturation of the environment with the injected gas after the first year of injection. The initial value was 11.5 MPa.

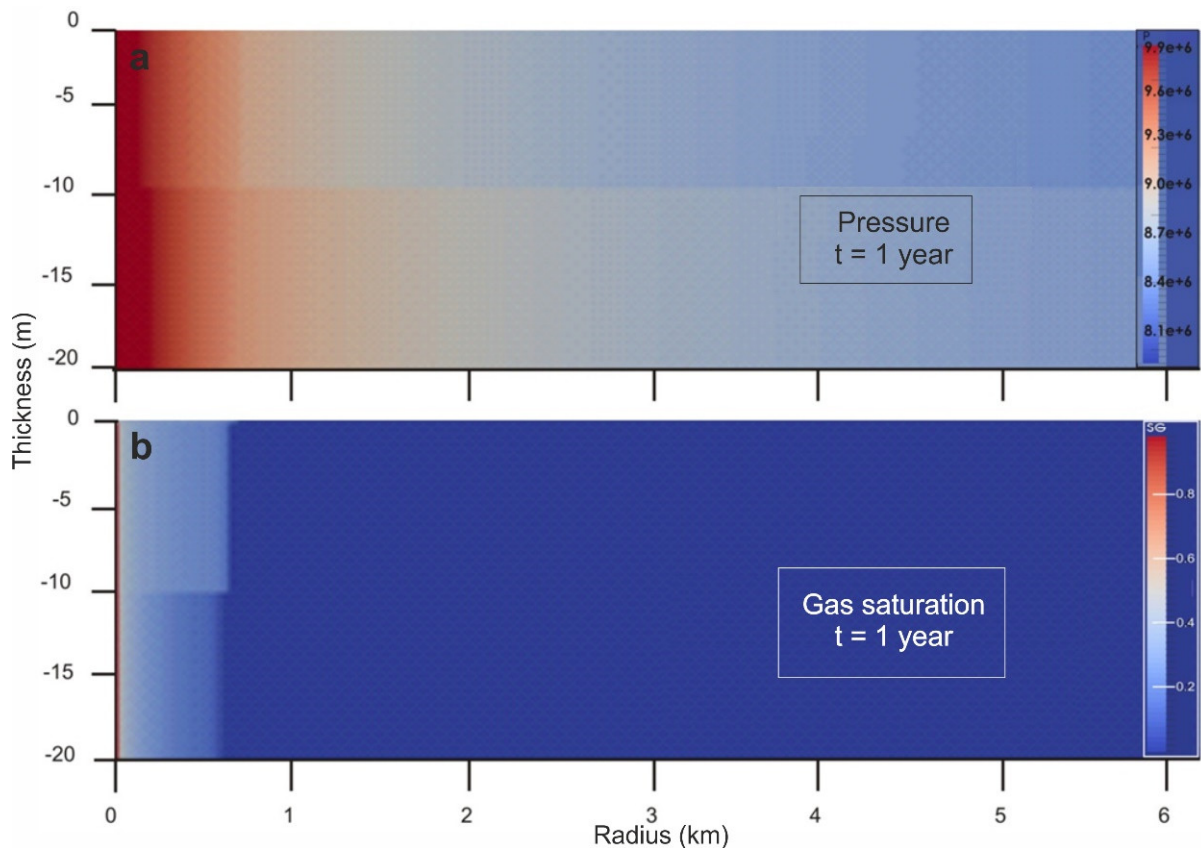


Figure 1. Evolution of the pressure (unit Pa) in the reservoir (a) and the gas saturation (forehead of plume of the injected CO₂) in the first year after injection (scale of the value of the CO₂ in the porous medium) (b). CO₂ injection started at point 0 on both the x-axis and y-axis.

In the first year of CO₂ injection, the pressure had a steady value of 9.96 MPa in the immediate surroundings of the injection. Despite the pressure decrease against the original value, the CO₂ pressure in the reservoir increases within the entire length of the model profile after one year of the injection. The highest value of 9.96 MPa was reached within the first 200 to 500 m from the injection borehole (Figure 1a). Furthermore, within the length of the model profile, the pressure has the value of 8.4 MPa with increasing distance from the injection borehole.

The pore environment of the reservoir was saturated with gas after the first year of CO₂ injection within a distance of 600 m. Maximum values of 50% of the value of the modelled supercritical pressure SG ($P_{\text{CO}_2} = 116$ bar) were achieved in the immediate vicinity of the injection borehole (Figure 1b).

Figure 2 shows the evolution of CO₂ pressure in the reservoir and the saturation of the environment injected with gas after 6 years of injection. Figures 1 and 2 show an increasing radius with respect to the injection well.

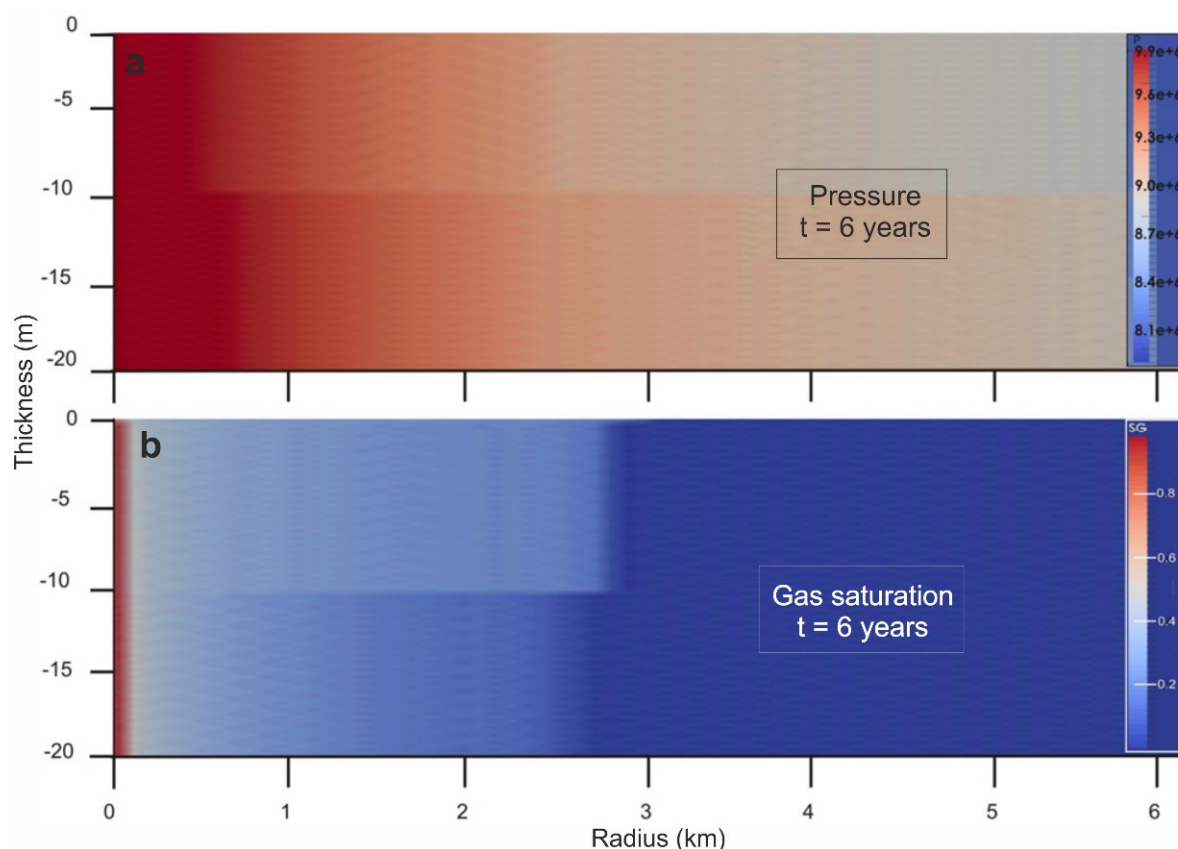


Figure 2. Evolution of the pressure (unit Pa) in the reservoir (a) and the gas saturation (forehead of the plume of the injected CO₂) after 6 years of injection (scale of the values of CO₂ in the porous medium) (b). CO₂ injection started at point 0 on both the x-axis and y-axis.

After 6 years, an injection pressure of 9.9 MPa was found within a distance of 1 km from the injection borehole (Figure 2a). Within a distance of 2.2 km, the structural pressure was equal to 9.4 MPa. In the remaining length of the model profile, the pressure value with increasing distance from the injection site drops to 9.0 MPa (Figure 2a). The saturation of the pore environment of the reservoir extends to about 2.7 km from the injection borehole after 6 years of injection. Maximum values of 100% of the modelled supercritical pressure SG ($P_{\text{CO}_2} = 116$ bar) were reached within the first tens of meters from the borehole (Figure 2b).

Figure 3 shows the saturation of the environment with the injected gas 100 and 500 years after the injection. After 100 years, the saturation of the pore environment by the gas at the top of the reservoir increases to almost 6 km (Figure 3a). On the contrary, at the base of the reservoir, the gas saturation is minimal (Figure 3a). After 500 years of structure relaxation, the loss of saturation in the pore environment due to dissipation of the gas (Figure 3b) is evident throughout the model profile.

Figure 4 presents a model representing the amount of dissolved CO₂ in a reservoir with a growing radius from the injection borehole and a relaxation time of 100 years (Figure 4a) and 500 years (Figure 4b) from injection. The solubility of CO₂ is almost constant, so CO₂ (aq) is in thermodynamic equilibrium with the surrounding brackish water at a concentration of 60.26 gCO₂/kg_{brine} throughout the structure that the cloud of injected CO₂ passed through. It can also be concluded that the amount of CO₂ (aq) in the pore environment of the storage structure decreases with increasing relaxation time (Figure 4).

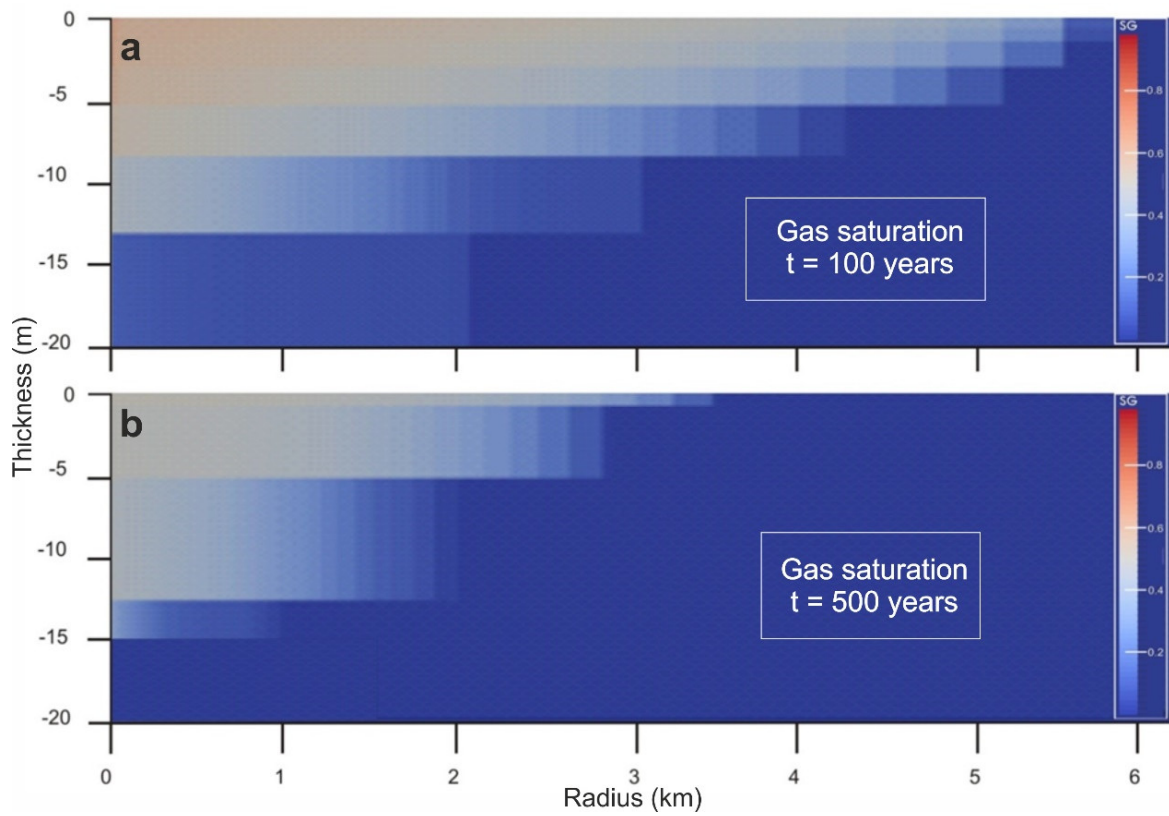


Figure 3. Saturation of the storage reservoir by CO₂ 100 (a) and 500 (b) years after the injection ceased. The scale on the right shows the CO₂ fraction values in the pore environment of the reservoir.

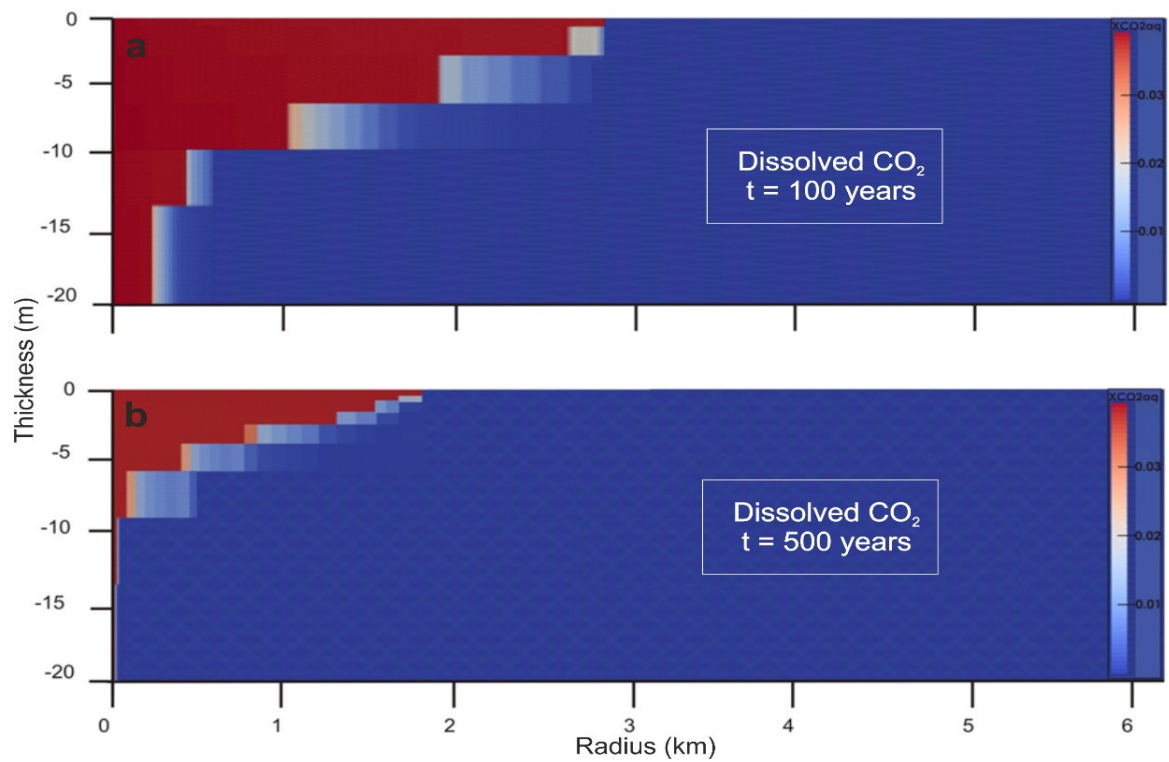


Figure 4. The amount of dissolved CO₂ in the reservoir 100 (a) and 500 (b) years after the injection ceased. The scale on the right shows the amount of CO₂ (aq).

The differences in permeability strongly affected the kinetics of saturation at depth, as shown by the coarser pressure and saturation changes in z-axis compared to x-axis after CO₂ injection ceased (Figures 1–4).

3.3. Modelled Mineralogical Changes in the Rock Mass Storage after the Injection of CO₂

Geochemical simulations of mineralogical rock changes in a potential CO₂ storage site were carried out using a batch simulation method. Batch simulation allows the performance of numerous successive simulation runs. They were used to explore the parameter space of a model or to optimize a set of model parameters. Thermodynamic data for individual rock-forming minerals and Portland cement (borehole grouting) were determined using the THERMOCHEM database [25]. These data consist of thermodynamic equilibria and saturation indices. Not all mineral phases forming the rock of the reservoir rock of the potential storage are listed in the used chemical database. Furthermore, the model does not distinguish between microcline and orthoclase, so if microcline is transformed into orthoclase after a reaction with acidified brackish water, this change will not be reflected in the model. However, a decrease or increase in the concentration of a given mineral due to ongoing reactions can be observed. However, this process is not expected. It is impossible to transform microcline into orthoclase in the testing conditions. These processes can only occur in metamorphic and igneous systems. Acidification of microcline is hydrolyzing microcline into clays. Kaolinite, siderite, and magnesite were not identified in the real rock sample Br-52, yet they are accounted for in the model. Clay minerals are a typical product of weathering, and kaolinite was chosen as their most common representative. Siderite was selected as a possible secondary phase, binding iron ions from solution. Precipitation of magnesite was assumed in the case of enrichment of the solution with magnesium. However, the formation of these secondary phases can only be expected if the pH of the brackish water solution increases again.

The kinetic parameters (the kinetic constant for 25 °C; the activation energy of the reaction; the degree of the reaction mechanism; the reactive surface of the mineral) of primary and secondary minerals used in model simulations have been taken from the literature data [20,28–30]. Table 7 shows all the mineral phases that were calculated in the model.

Table 7. Mineral phases used in the model.

Mineral	Formula
Quartz	SiO ₂
Muscovite	KAl ₂ (AlSi ₃)O ₁₀ (OH) ₂
Microcline	KAlSi ₃ O ₈
Chlorite	Fe ₅ Al(AlSi ₃)O ₁₀ (OH) ₈
Calcite	CaCO ₃
Siderite	FeCO ₃
Dolomite	CaMg(CO ₃) ₂
Albite	NaAlSi ₃ O ₈
Kaolinite	Al ₂ Si ₂ O ₅ (OH) ₄
Gypsum	CaSO ₄ ·2H ₂ O
Magnesite	MgCO ₃
CSH1.6	Ca _{1.6} SiO _{3.6} ·2.58H ₂ O
Portlandite	Ca(OH) ₂
Ettringite	Ca ₆ Al ₂ (SO ₄) ₃ (OH) ₁₂ ·26H ₂ O
Hydrotalcite	Mg ₄ Al ₂ O ₇ ·10H ₂ O
Katoite-Si	Ca ₃ Al ₂ SiO ₄ (OH) ₈
C3FH6	Ca ₃ Fe ₂ (OH) ₁₂

The input parameters for modeling mineralogical changes in fluid-bearing rock and borehole grouting are as follows: the chemical composition of brackish water Br-45 (Table 6), the mineralogical composition (in vol.%) and porosity (in%) of real studied rock samples (Table 3), and of Portland cement (see Table 4). Porosity changes were quantified from mass

balance. The injected amount of CO₂ was assumed to be 8750 tCO₂/year, corresponding to an injection rate of 0.28 kgCO₂/s.

pH is the key to phase stability. At a distance of 20 m from the injection well, a sharp drop in pH will occur in the storage structure in the first year of injection. In the first months, the pH of the brackish water used in the modeling is relatively stable at its original value of 8.1. In the third and fourth months, the pH will drop for the first time to a value of around 6.4. This may be due to the dissolution of gypsum and calcite. The buffering capacity of the reservoir rock decreases. After 6 months, when the system was buffered with carbonate substances contained in the solution and the pH value dropped from 6.4 to only 6.2, there will be a further drop in pH to 4.5. The pH then decreases slightly until the end of the first year of injection, when it reaches a value of 4.2 at a distance of 20 m from the injection well.

After the end of CO₂ injection into the reservoir rock of the potential storage at a distance of 20 m from the injection well, the pH will rise very quickly to the value of 7. The maximum value of pH 7.3 will be reached after about 100 years. Subsequently, it slowly decreases again. The reasons for this decrease may be the same reactions that led to the decrease in pH near the injection well. Thus, it may be related to the release of residual CO₂ trapped in the structural pastes, to the dissolution of magnesite, or to both processes simultaneously. After about 350 years, the pH value drops to a final value of 6.4 and does not develop further.

Mineralogical changes in the reservoir rock at 20 m from the injection borehole over 8 years of storage operation are shown in Figure 5a. The model shows that, about 4 years after injection, the dolomite and the microcline are slightly decreasing. Microcline decreased right away, but it began to stagnate from the fourth year. The brackish water is enriched with magnesium, which leads to the precipitation of magnesite. After 6 years, calcite and gypsum dissolve slightly, releasing calcium, carbonate, and sulfate ions. Quartz, albite, chlorite, and muscovite remained stable throughout the storage operation.

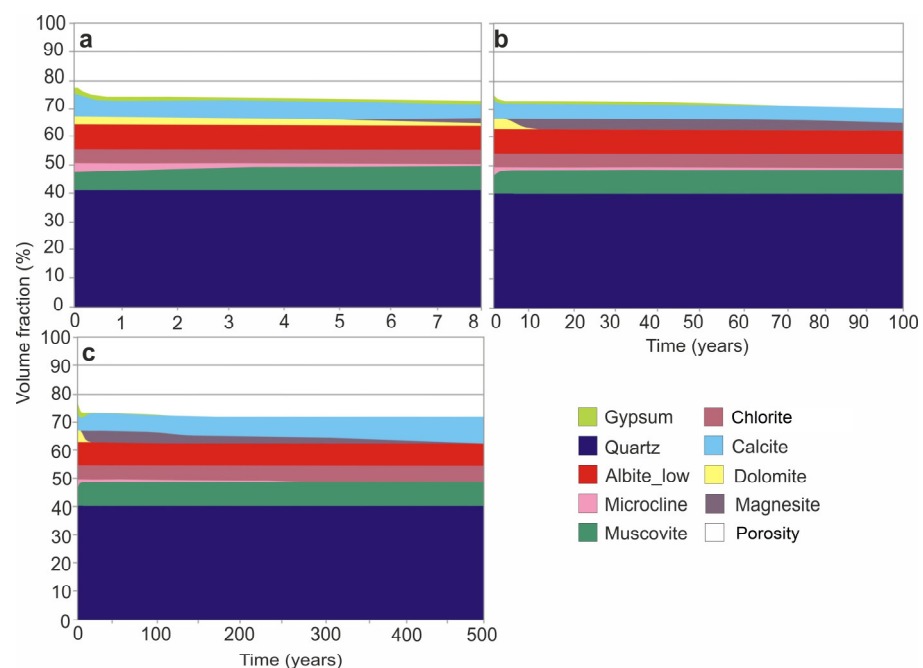


Figure 5. Mineralogical changes in the Br-52 rock sample over 8 years of injection (a) and after 100 years (b) and 500 years (c) from the completion of injection at a distance of 20 m from the injection borehole.

Five years after injection was completed, dolomite was completely dissolved (Figure 5b) and replaced with magnesite. After 60 years, the gypsum was dissolved completely, and the calcite was slightly dissolved. Calcite enters the model with a higher volume% value

than dolomite. Calcite generally has faster kinetics than dolomite, but it also depends on the mass balance of both minerals and environmental conditions. The brackish water is saturated with Ca^{2+} and HCO_3^- ions during the dissolution of both minerals. As a result of the dissolution of other phases, the brackish water may become oversaturated with calcium and bicarbonates. Secondary calcite will form, as in this case.

One hundred years after injection, a decrease in magnesite is evident (Figure 5b). This may be related to the pH variation in the reservoir rock. Dissolving magnesite not only releases magnesium, but also carbonate ions that can bind to protons and increase pH.

At a higher pH, calcite is precipitated again after about 200 years, as can be seen in Figure 5c. After 250 years, the microcline is completely dissolved, and the clay minerals of the chlorite groups are precipitated. The other minerals are stable even 500 years after injection (Figure 5c).

The model shows an increase in porosity during injection (Figure 5a) from the original 24.5% to 27%. The porosity slightly decreases after CO_2 injection (26.5%) and slightly increases over 100 years of relaxation to a value of 29% (Figure 5b). After 200 years, porosity slightly decreases to a value of 28.5%, and for the next 300 years it stagnates at a given value (Figure 5c). The decreasing porosity may be associated with the precipitation of calcite and chlorite group clay minerals. This is volumetrically overcompensating dissolution.

The composition of the cement in vol.% grouting of the injection borehole is described in Table 4. It is typical of Portland cement.

Experiments confirm the rapid dissolution of portlandite and its replacement by calcite. The Ca–Si hydrate (CSH) gel is also dissolved, and silica gel (i.e., silica) appears. Porosity decreases slowly in the first few years of injection, mainly due to the precipitation of calcite.

After the completion of injection, the CSH gel is completely dissolved and is replaced by precipitates of calcite and silica (Figure 6a).

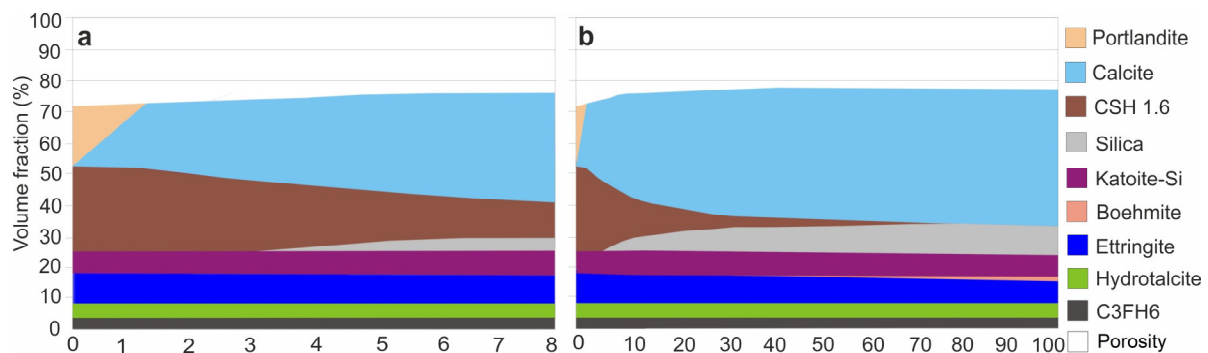


Figure 6. Mineralogical changes in Portland cement over 8 years of CO_2 injection (a) and over the 100 years after the completion of injection (b).

Katoite and hydrotalcite also dissolve. These processes are slower and contribute to the formation of Al gels (i.e., boehmite). The porosity of the cement drops after the end of CO_2 injection, dropping from the original value of 28% to 22% after 100 years of relaxation time (Figure 6b).

4. Conclusions

The TOUGHREACT program was used to simulate the geochemical reactions of injected CO_2 , with the aim to predict gas distribution through the rocks bearing the brackish water during the injection (1 and 6 years) and in the 100 and 500 years of relaxation.

It was found that the CO_2 pressure in the reservoir increases within the entire length of the model profile after one year of grouting, reaching 9.96 MPa in the first 200 m from the injection borehole. Furthermore, within the length of the model profile (6 km), the pressure drops with increasing distance from the injection borehole to a value of 8.4 MPa. The pore environment of the reservoir is saturated with gas after the first year of CO_2 injection only.

within a distance of 600 m. After 6 years, an injection pressure of 9.9 MPa was found within a distance of 1 km from the injection borehole. Within a distance of 2.2 km, the structure pressure is equal to 9.4 MPa.

For the remaining length of the model profile, the pressure drops with increasing distance from the injection site to a value of 9.0 MPa. The pore saturation of the reservoir rock is extended to about 2.7 km from the injection borehole after 6 years of injection. Maximum values of 100% of the value of the modelled supercritical pressure SG ($P_{CO_2} = 116$ bar) were reached within the first tens of meters from the borehole.

One hundred years after injecting, the pore saturation by the gas at the top of the reservoir increased to almost 6 km away. On the contrary, at the base of the reservoir, the saturation of the gas is minimal, and after 500 years of structure relaxation, there is a noticeable loss of pore saturation by the gas within the whole model profile. It is also evident that the amount of $CO_2(aq)$ in the pore environment of the storage site structure decreases with increased relaxation time. Similar conclusions were reached by other authors [9,13] who were involved in modeling the spread of injected CO_2 into the structure of sedimentary rocks.

Interactions were also studied in the CO_2 –rock–brackish water system (models were made for reservoir rock). The aim was to characterize the influence of CO_2 in the geological structure on mineralogical rock changes from the potential storage site.

For reservoir rocks, the most important chemical processes are the dissolution of carbonates (calcite and dolomite) and microcline due to acidification of the brackish water during the injection of CO_2 into the structure. The dissolution of some mineral phases during the injection and the increase in porosity in the structure affect the sequestration capacity of the reservoir rock of the potential storage site. The dissolution of carbonates and microcline was also confirmed in their study by Wang et al. (2019) [6]. In her study, Gaus et al. (2008) [9] describes the importance of the dissolution of mineral phases for the increased storage capacity of the reservoir rock. The results of the presented work are in agreement with the conclusions of these authors.

Other chemical processes that the models describe include the precipitation of magnesite, which replaces dissolving dolomite completely, and the formation of secondary carbonates as a result of the increasing pH of the brackish water in the structure over a longer period of time after injection is ceased. Carbonate minerals bind CO_2 to their structure and help to stabilize the pH of the brackish water after injecting. The consequence of this process is, however, the reduction in the porosity of the reservoir rock. Klunk et al. (2020) [31] also observed the precipitation of magnesite in his work at elevated pressure-temperature and high salinity.

In the long term, these processes are desirable. The formation of secondary phases is considered useful during the relaxation period of the deposit after CO_2 injection [1,4]. The newly formed phases close the injected CO_2 in the structure and thus contribute to the stability of the environment. They also represent a barrier for possible CO_2 leaks into the caprock [5,6].

The porosity of reservoir rock increases by 4% during the model period, i.e., after 8 years of injecting and then 500 years of structure relaxation.

Experiments in the CO_2 –cement–brackish water system were carried out in order to determine and describe the degradation of the cement grouting of the borehole. The models confirm the rapid dissolution of portlandite and its replacement with calcite. Kutchko et al. (2007) [32] conducted laboratory experiments of well cement degradation by CO_2 -rich brine under geological (P, T) conditions and proposed a degradation mechanism for Portlandite. Indeed, CO_2 -rich acid brine dissolves Portlandite $Ca(OH)_2$ and precipitates Calcite $CaCO_3$. The CSH gel is also dissolved, and silica gel (i.e., silica) appears. Porosity decreases quickly in the first few years, mainly due to the precipitation of calcite. After completion of the injection, the CSH gel is completely dissolved, replaced by the precipitation of calcite and silica. Other authors [33,34] have come to the same conclusion. In their papers they also describe the decalcification of the CSH phases, and that CO_2 mainly affects the initial phases

of the cement: portlandite, CSH and aluminates. In addition, carbonation is complete and leads to the formation of amorphous silicates. Katoite and hydrotalcite also dissolve. These processes are slower and contribute to the formation of Al gels (i.e., boehmite). The porosity of the cement after the cessation of CO₂ injection continues to decrease, dropping from the original value of 28% to 22% over 100 years of relaxation. Mineral changes are very obvious. The deterioration of the sealing capacity of the borehole grouting and the potential risks of CO₂ leakage through the borehole casing are evident precisely because of the mineral changes and the speed of these processes, especially during the first years of CO₂ injection. Experiments by Jobard (2013) [19] show that the cement structure is nevertheless maintained, and so might not endanger the tightness of the cement. It is therefore necessary to carry out further studies on such a cement slurry and to prevent the possibility of mechanical damage to the integrity of the borehole.

Immediately after its injection, CO₂ spreads in its supercritical form and partially dissolves into the groundwater [1]. This process significantly changes mineralogical, hydrogeological, and geochemical conditions at the storage site [2–4]. It acidifies the original groundwater of the brackish water type; it can influence hydrogeological parameters, especially the porosity and permeability of the deposit rock; it changes the mineralogical composition of the deposit rock and can mineralogically affect the confining layers in the overburden; and it causes chemical changes in the cement grouting of the borehole [2–6]. All these reactions can be a potential risk for the CO₂ storage process in the selected structure and can lead to CO₂ leakage from the deposit to the surface [7,8]. It is therefore necessary to understand the mechanism of these reactions and to quantify and evaluate them to ensure the safety and sustainability of storage [1,4,6].

Author Contributions: Conceptualization, M.L.; methodology, M.L.; software, M.L.; validation, M.L. and N.R.; formal analysis, M.L.; investigation, M.L.; resources, M.L., L.M.; data curation, M.L., L.M.; writing—original draft preparation, M.L.; writing—review and editing, K.S., N.R.; visualization, M.L.; supervision, N.R.; project administration, K.S.; funding acquisition, N.R., M.L. All authors have read and agreed to the published version of the manuscript.

Funding: This research was funded by project of SGS No. SV5412211/2101, Faculty of Mining and Geology, VSB—Technical University of Ostrava, Czech Republic.

Data Availability Statement: Not applicable.

Conflicts of Interest: The authors declare no conflict of interest.

References

1. Gaus, I. Role and impact of CO₂–rock interactions during CO₂ storage in sedimentary rocks. *Int. J. Greenh. Gas Control* **2010**, *4*, 73–89. [CrossRef]
2. Yasuhara, H.; Elsworth, D.; Polak, A. Evolution of permeability in a natural fracture: Significant role of pressure solution. *J. Geophys. Res. Atmos.* **2004**, *109*, 1–11. [CrossRef]
3. Zhang, L.; Wang, Y.; Miao, X.; Gan, M.; Li, X. Geochemistry in geologic CO₂ utilization and storage: A brief review. *Adv. Geo-Energy Res.* **2019**, *3*, 304–313. [CrossRef]
4. Ajayi, T.; Gomes, J.S.; Bera, A. A review of CO₂ storage in geological formations emphasizing modeling, monitoring and capacity estimation approaches. *Pet. Sci.* **2019**, *16*, 1028–1063. [CrossRef]
5. Foroutan, M.; Ghazanfari, E.; Amirlatifi, A. Variation of failure properties, creep response and ultrasonic velocities of sandstone upon injecting CO₂-enriched brine. *Géoméch. Geophys. Geo-Energy Geo-Resour.* **2021**, *7*, 27. [CrossRef]
6. Wang, Y.; Zhang, L.; Soong, Y.; Dillmore, R.; Liu, H.; Lei, H.; Li, X. From core-scale experiment to reservoir-scale modeling: A scale-up approach to investigate reaction-induced permeability evolution of CO₂ storage reservoir and caprock at a U.S. CO₂ storage site. *Comput. Geosci.* **2019**, *125*, 55–68. [CrossRef]
7. Kaszuba, J.P.; Janecky, D.R.; Snow, M.G. Experimental evaluation of mixed fluid reactions between supercritical carbon dioxide and NaCl brine: Relevance to the integrity of a geologic carbon repository. *Chem. Geol.* **2005**, *217*, 277–293. [CrossRef]
8. Labus, K.; Bujok, P. CO₂ mineral sequestration mechanisms and capacity of saline aquifers of the Upper Silesian Coal Basin (Central Europe)—Modeling and experimental verification. *Energy* **2011**, *36*, 4974–4982. [CrossRef]
9. Gaus, I.; Audigane, P.; André, L.; Lions, J.; Jacquemet, N.; Durst, P.; Azaroual, M. Geochemical and solute transport modelling for CO₂ storage, what to expect from it? *Int. J. Greenh. Gas Control* **2008**, *2*, 605–625. [CrossRef]

10. Zhou, B.; Liu, L.; Zhao, S.; Ming, X.-R.; Oelkers, E.H.; Yu, Z.-C.; Zhu, D.-F. Dawsonite formation in the Beier Sag, Hailar Basin, NE China tuff: A natural analog for mineral carbon storage. *Appl. Geochem.* **2014**, *48*, 155–167. [[CrossRef](#)]
11. Marty, N.C.; Tournassat, C.; Burnol, A.; Giffaut, E.; Gaucher, E.C. Influence of reaction kinetics and mesh refinement on the numerical modelling of concrete/clay interactions. *J. Hydrol.* **2009**, *364*, 58–72. [[CrossRef](#)]
12. Radvanec, M.; Tuček, L.; Čechovská, K.; Derco, J.; Kucharič, L. Permanent disposal of CO₂ industrial emission via artificial carbonatization of metaperidotite, metawehrlite and metawebsterite: An experimental study. *Slovak. Geol. Mag.* **2008**, *53*, 65.
13. Wertz, F.; Vrbová, V.; Havlová, V. Numerical Simulations of Supercritical Injection of CO₂ in Dunajovice Sandstone. *Fuels* **2014**, *6*, 108–115. [[CrossRef](#)]
14. Brandl, A.; Cutler, J.; Seholm, A.; Sansil, M.; Braun, G. Cementing Solutions for Corrosive Well Environments. *SPE Drill. Complet.* **2011**, *26*, 208–219. [[CrossRef](#)]
15. Bujok, P.; Grycz, D.; Klempa, M.; Kunz, A.; Porzer, M.; Pytlik, A.; Rozehnal, Z.; Vojčinák, P. Assessment of the influence of shortening the duration of TRT (thermal response test) on the precision of measured values. *Energy* **2014**, *64*, 120–129. [[CrossRef](#)]
16. Wertz, F.; Gherardi, F.; Blanc, P.; Bader, A.-G.; Fabbri, A. Cement CO₂-alteration propagation at the well–caprock–reservoir interface and influence of diffusion. *Int. J. Greenh. Gas Control* **2013**, *12*, 9–17. [[CrossRef](#)]
17. Fetter, C.W. *Applied Hydrogeology*, 4th ed.; Prentice-Hall, Inc.: Hoboken, NJ, USA, 2001; p. 598, ISBN 0-13-088239-9.
18. Appelo, C.A.J.; Postma, D. *Geochemistry, Groundwater and Pollution*, 2nd ed.; A.A. Balkema Publishers: Leiden, The Netherlands, 2005; p. 635, ISBN 04 1536 421 3.
19. Jobard, E. Modélisation Expérimentale du Stockage Géologique de CO₂, Étude Particulière des Interfaces Entre le Ciment de Puits, la Roche Couverture et la Roche Reservoir. Ph.D. Thesis, The National Polytechnic Institute of Lorraine INPL, Nancy, Lorraine, France, 2013.
20. Baur, I.; Keller, P.; Mavrocordatos, D.; Wehrli, B.; Johnson, C. Dissolution-precipitation behaviour of ettringite, monosulfate, and calcium silicate hydrate. *Cem. Concr. Res.* **2004**, *34*, 341–348. [[CrossRef](#)]
21. Pruess, K. *ECO_{2n}: A TOUGH2 Fluid Property Module for Mixtures of Water, NaCl and CO₂*; Lawrence Berkeley National Laboratory Report (No. LBNL-57952); Lawrence Berkeley National Laboratory: Berkeley, CA, USA, 2005.
22. Pruess, K.; Oldenburg, C.M.; Moridis, G.J. *TOUGH2 User's Guide, Version 2.0*; Lawrence Berkeley National Laboratory Report (No. LBNL-43134); Lawrence Berkeley National Laboratory: Berkeley, CA, USA, 1999.
23. Bethke, C.M. *The Geochemist's Workbench, Release 6.0—Reference Manual*; University of Illinois: Springfield, IL, USA, 2006.
24. Parkhurst, D.L.; Appelo, C.A.J. *Description of Input and Examples for PHREEQC Version 3-A Computer Program for Speciation, Batch-Reaction, One-Dimensional Transport, and Inverse Geochemical Calculations*; U.S. Geological Survey Techniques and Methods; U.S. Geological Survey: Menlo Park, CA, USA, 2013; pp. 1–497. Available online: <https://pubs.usgs.gov/tm/06/a43/> (accessed on 20 October 2022).
25. Piantone, P.; Nowak, C.; Blanc, P.; Lassin, A.; Burnol, A. *THERMODDEM: Thermodynamique et Modélisation de la Dégradation des Dechets Minéraux. Report D'avancement*; BRGM/RP-54547-FR; Bureau de Recherches Géologiques et Minières: Orléans, France, 2006; p. 51.
26. Blanc, P.; Lassin, A.; Piantone, P.; Azaroual, M.; Jacquemet, N.; Fabbri, A.; Gaucher, E. Thermoddem: A geochemical database focused on low temperature water/rock interactions and waste materials. *Appl. Geochem.* **2012**, *27*, 2107–2116. [[CrossRef](#)]
27. Stumm, W.; Morgan, J.J. *Aquatic Chemistry: Chemical Equilibria and Rates in Natural Waters*; John Wiley & Sons: New York, NY, USA, 1995; p. 1022, ISBN 0-471-51184-6.
28. Galí, S.; Ayora, C.; Alfonso, P.; Tauler, E.; Labrador, M. Kinetics of dolomite–portlandite reaction: Application to Portland cement concrete. *Cem. Concr. Res.* **2001**, *31*, 933–939. [[CrossRef](#)]
29. Palandri, J.L.; Kharaka, Y.K. *A Compilation of Rate Parameters of Water-Mineral Interaction Kinetics for Application to Geochemical Modeling (Open File Report 2004-1068)*; U.S. Geological Survey: Menlo Park, CA, USA, 2004.
30. Schweizer, C.R. Calciumsilikathydrat-Mineralien. Lösungskinetik und ihr Einfluss auf das Auswaschverhalten von Substanzen aus einer Ablagerung mit Rückständen aus Müllverbrennungsanlagen. Ph.D. Thesis, Universität Basel, Basel, Switzerland, 1999.
31. Klunk, M.A.; Shah, Z.; Caetano, N.R.; Conceição, R.V.; Wander, P.R.; Dasgupta, S.; Das, M. CO₂ sequestration by magnesite mineralisation through interaction of Mg-brine and CO₂: Integrated laboratory experiments and computerised geochemical modelling. *Int. J. Environ. Stud.* **2020**, *77*, 492–509. [[CrossRef](#)]
32. Kutchko, B.G.; Strazisar, B.R.; Dzombak, D.A.; Lowry, G.V.; Thaulow, N. Degradation of Well Cement by CO₂ under Geologic Sequestration Conditions. *Environ. Sci. Technol.* **2007**, *41*, 4787–4792. [[CrossRef](#)] [[PubMed](#)]
33. Carey, J.W.; Wigand, M.; Chipera, S.J.; Woldegabriel, G.; Pawar, R.; Lichtner, P.C.; Wehner, S.C.; Raines, M. A.; Gut-hrie., G.D., Jr. Analysis and performance of oil well cement with 30 years of CO₂ exposure from the SACROC Unit, West Texas, USA. *Int. J. Greenh. Gas Control.* **2007**, *1*, 75–85. [[CrossRef](#)]
34. Jacquemet, N.; Pironon, J.; Saint-Marc, J. Mineralogical Changes of a Well Cement in Various H₂S-CO₂(-Brine) Fluids at High Pressure and Temperature. *Environ. Sci. Technol.* **2008**, *42*, 282–288. [[CrossRef](#)] [[PubMed](#)]

Disclaimer/Publisher's Note: The statements, opinions and data contained in all publications are solely those of the individual author(s) and contributor(s) and not of MDPI and/or the editor(s). MDPI and/or the editor(s) disclaim responsibility for any injury to people or property resulting from any ideas, methods, instructions or products referred to in the content.